

Analysis of GPS ionospheric scintillation signal amplitude fading characteristics at low latitude

Zhu Xuefen^{1,2} Chen Xiyuan^{1,2} Huang Haoqian^{1,2} Chen Jianfeng³ Xu Bincheng^{1,2}

(¹ School of Instrument Science and Engineering, Southeast University, Nanjing 210096, China)

(² Key Laboratory of Micro-Inertial Instrument and Advanced Navigation Technology of Ministry of Education, Southeast University, Nanjing 210096, China)

(³ Automotive Engineering Research Institute, Jiangsu University, Zhenjiang 212013, China)

Abstract: The received satellite signal amplitude is attenuated greatly due to the strong ionospheric scintillation for low latitude regions, which causes the GPS tracking loop's loss of lock, the positioning errors to increase, and navigation to be interrupted. To solve the above problems, a novel signal processing algorithm is proposed based on the GPS L1 software receiver during strong ionospheric scintillation using the multi-channel intermediate frequency (IF) data sampling system. Tens of thousands of fading events are obtained based on the signal intensity measurement. The amplitude fading characteristics in the low latitude region are analyzed, including fading duration, time separation between fades and the numbers of signal intensity fading events. The fading thresholds are set to be 15 and 10 dB, respectively. The main fading time is very short in -15 dB fading threshold, which generally is less than 20 ms. The main time separation between fades is less than 2 s in a single one-hour period from the time 23:00 to 24:00. Therefore, it has the characteristic of a short reacquisition time for the receiver designed to reduce the probability of simultaneous loss of lock for some satellites. Subsequently, the acquisition, tracking and PVT (position, velocity and time) calculations are completed by the custom-designed software receiver. The results show that the impact analysis of ionospheric scintillation on GPS amplitude attenuation in the low latitude region is helpful for designing the advanced tracking algorithm and to improve the robustness and accuracy of the GPS receiver.

Key words: GPS L1; ionospheric scintillation; amplitude fading characteristics

DOI: 10.3969/j.issn.1003-7985.2016.04.015

The ionospheric scintillation will cause the signal amplitude's deep fading and the phase's sharp fluctuation

when the GPS signal passes through the ionospheric irregularities. In the mid-latitude region, the ionospheric amplitude and the phase scintillation are usually not observed. However, in the low-latitude region close to the equator, particularly in the period of solar maximum after sunset, the ionospheric scintillation is often observed and it restricts the GPS navigation^[3-4]. The GPS signal received can be attenuated more than 30 dB due to strong scintillation, and it has a great impact on receiver carrier tracking, estimation accuracy, availability, and integration of GPS position, velocity and time (PVT) solutions^[5-6].

There have been many studies on the effect of scintillation on the GPS L1 signal^[7-8] until now. However, these studies are based on commercial receivers and focus on how GPS navigation solutions were influenced by the ionospheric scintillation. The commercial receiver is limited to resources and the signal fade cannot be explored in depth. The interior of the software receiver is analyzed, including fading duration, and the time separation between fades. It is very useful to improve the robustness of GPS receivers under the condition of scintillation. The previous research concerns the fading features based on carrier-to-noise ratio (C/N_0)^[6], and the fading features based on measurements of signal intensity are analyzed in this paper. Besides, the ionospheric scintillation data used in Ref. [6] was collected on Ascension Island in 2001, and the data used in this paper was collected in 2013 in Brazil closest to the solar maximum year.

High-rate signal intensity measurements are analyzed using the data sampled by a GPS multi-channel data collection system deployed at São José dos Campos, Brazil (23.2 S, 45.9 W) in November, 2013, which is a solar maximum year at a low-latitude site. A GTEC[®] free front-end is used to record the GPS IF signals. The front-end generates zero IF data streams with 8-bit resolution I/Q samples at 20 MHz complex sampling rate for GPS L1 band. Then the data is processed by a customized software defined receiver (SDR) to obtain signal intensity measurements. The fading features, which includes fading duration, time separation between fades and the numbers of signal intensity fading events, are analyzed by

Received 2016-06-15.

Biography: Zhu Xuefen (1983—), female, doctor, associate professor, zhuxuefen@seu.edu.cn.

Foundation items: The National Natural Science Foundation for Young Scholars (No. 51405203), Jiangsu Overseas Research and Training Program for University Prominent Young and Middle-Aged Teachers and Presidents, the Natural Science Foundation of Jiangsu Province (No. BK20160699).

Citation: Zhu Xuefen, Chen Xiyuan, Huang Haoqian, et al. Analysis of GPS ionospheric scintillation signal amplitude fading characteristics at low latitude[J]. Journal of Southeast University (English Edition), 2016, 32(4): 484 – 488. DOI: 10.3969/j.issn.1003-7985.2016.04.015.

setting the fading threshold to be -15 and -10 dB in the signal intensity measurements.

1 Definition of S_4 , S_1 and C/N_0 Index

The S_4 index represents the fluctuation of the signal intensity (SI) ^[9–10].

$$W_{BP} = \sum_{i=1}^M (I_i^2 + Q_i^2) \quad (1)$$

$$N_{BP} = \left(\sum_{i=1}^M I_i \right)^2 + \left(\sum_{i=1}^M Q_i \right)^2 \quad (2)$$

where M represents the number of I_i^2 and Q_i^2 which are used to generate the wide band power W_{BP} or the narrow band power N_{BP} measurement. The coherent integration is applied to the correlator outputs by moving the window accumulator for a long period of time to increase the accumulated signal energy. In the previous experiments with various accumulation time intervals^[11] for GPS L1 strong scintillation signals, it is shown that 40-block correlator outputs contain sufficient energy to obtain useful measurements and every 1 ms represents one block. Since the GPS navigation data rate is 50 Hz, the product of the M value and the coherent integration time is equal to the multiple of 20 ms to avoid the summation. The same interval of 40 ms is applied to GPS L1 band signal, and the M value is set to be 40 and I_i^2 , Q_i^2 are integrated over 1 ms.

$$S_{I, \text{raw}} = N_{BP} - W_{BP} \quad (3)$$

$$S_{I, \text{norm}} = \frac{S_{I, \text{raw}}}{S_{I, \text{trend}}} \quad (4)$$

where $S_{I, \text{raw}}$ is the raw signal intensity; $S_{I, \text{norm}}$ is the nor-

malized signal intensity (NSI), which is generated by using $S_{I, \text{raw}}$ and the low frequency trend $S_{I, \text{trend}}$; $S_{I, \text{trend}}$ is obtained by using the 4th-order polynomial fitting for $S_{I, \text{raw}}$. Amplitude scintillation that induces S_4 is calculated by using the normalized signal intensity $S_{I, \text{norm}}$.

$$S_4 = \sqrt{\frac{\langle S_{I, \text{norm}}^2 \rangle - \langle S_{I, \text{norm}} \rangle^2}{\langle S_{I, \text{norm}} \rangle^2}} \quad (5)$$

where $\langle \rangle$ represents the average value over the interval and the interval is 10 s in this paper.

The C/N_0 of the received GPS signal can be estimated by using the I/Q channel correlator outputs^[12]. The computationally efficient power ratio method is used to estimate C/N_0 as follows:

$$\mu = \frac{M}{K} \sum_{K=1}^{K/M} \frac{N_{BP, K}}{W_{BP, K}} \quad (6)$$

$$C/N_0 = 10 \lg \frac{\mu - 1}{T_{\text{int}} (M - \mu)} \quad (7)$$

where K is the number of samples in the average time interval of 1 s.

The impacts of strong scintillation on the normalized signal intensity, S_4 and C/N_0 for GPS PRN29 satellite are shown in Figs. 1 (a) to (c). The data is sampled from 0:00:01 using universal time coordinated (UTC) for 1 h on 18 November, 2013 in Brazil. In Fig. 1, NSI, S_4 and C/N_0 vary slowly without scintillation before reaching 1 400 s. However, when strong scintillation occurs after 1 400 s, NSI and S_4 fluctuate rapidly even exceeding 40 dB at times. $S_4 > 0.5$ indicates deep amplitude fading. It shows that many deep fades occurred in the GPS measurements.

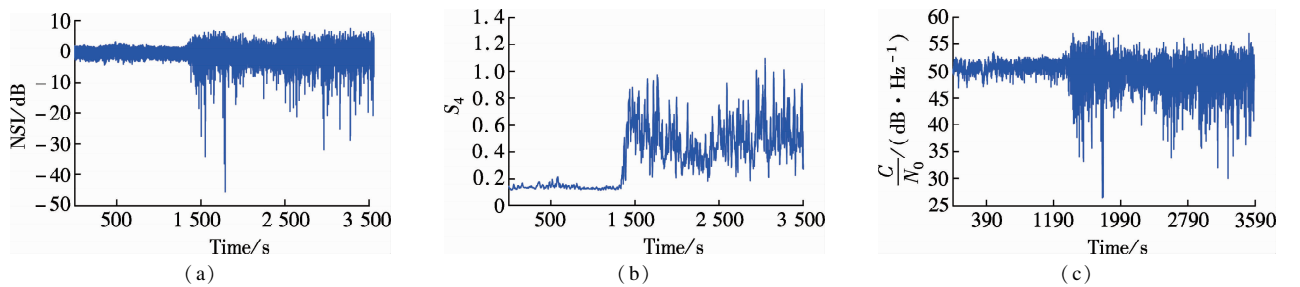


Fig. 1 The signal intensity of GPS L1 PRN29. (a) NSI; (b) S_4 ; (c) C/N_0

2 Fading Index Definition

From the data sampled at São José dos Campos, Brazil (23. 2S, 45. 9W), a large number of signal fading events have been extracted. The normalized signal intensity is used to calculate the fading indices including fading duration and time separation between fades^[13–14]. The normalized signal intensity is obtained using the 4th-order polynomial fitting method, so the nominal value is set to 0 dB. The fading threshold is set to be -15 dB to extract fading events from the datasets mentioned in the follow-

ing definition.

The fading duration is an important feature for receiver signal processing because it determines whether reacquisition is needed if the GPS signal experiences loss of lock, and it also has an impact on the accuracy of the PVT solutions if tracking is maintained. In Fig. 2, the fading duration is defined as the time difference between NSI declining below the threshold of 10 to 15 dB and NSI increasing above the threshold. Another fading index is the time separation between fades. The time separation between fades is defined as the time difference between the middle points of

two consecutive fades under the threshold. The time separation between fades has an influence on signal reacquisition and the carrier smoothing process of code measurements in receivers.

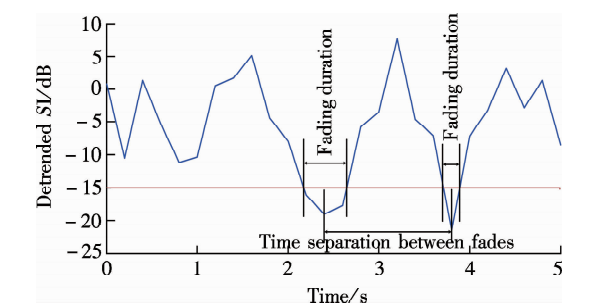


Fig. 2 Fading indices definition

3 Low-Latitude GPS Signal Intensity Fading Analysis

A GTEC[®] free front-end is used to record the GPS L1 IF signals with the influence of ionospheric scintillation in São José dos Campos, Brazil (23.2 S, 45.9 W) on November 18th, 2013. The IF data is post-processed to generate the scintillation observables. Two hours of data, collected from different PRNs with the universal time coordinated (UTC) starting times of 0:00:01 and 23:00:02 on November 18th, 2013, are analyzed. The two hours of data are shown in Tab. 1.

Tab. 1 Details of two hours of data collected

UTC starting time	PRNs in the first 60 s	PRNs in the final 60 s
0:00:01	12,25,29,31,21,5,2,15	25,29,12,21,5,18
23:00:02	29,2,12,25,5,24,10,21,31	25,12,29,21,5,31,2,15

Fig. 3 shows the distributions of GPS L1 fading duration of the signal intensity in Brazil under the thresholds of -15 dB. Different PRNs are labeled in the legends as the representatives. The scale of y-axis is the base -10 logarithmic diagram to show the details for points with small probabilities. It is noted that the distributions are discrete and the connecting lines are depicted to show the trend. The results indicate that the predominant fading durations are very short, typically less than 20 ms. In Figs. 3 (a) and (b), the unevenness duration is more than 60 ms, and the unevenness duration also restricts the numbers of fading events.

Fig. 4 shows the distributions of GPS L1 time separation between fades of the signal intensity under the thresholds of -15 dB. Different PRNs are labeled in the legends as the representatives. The y-axis shows the value of the logarithmic diagram. The results show the distribution shape of time separations observed when the UTC starting time is 0:00:01 and 23:00:02, but also that the predominant time separation between fades is shorter when the UTC starting time is 23:00:02, usually less than 2 s. Fading duration and time separation between fades are two

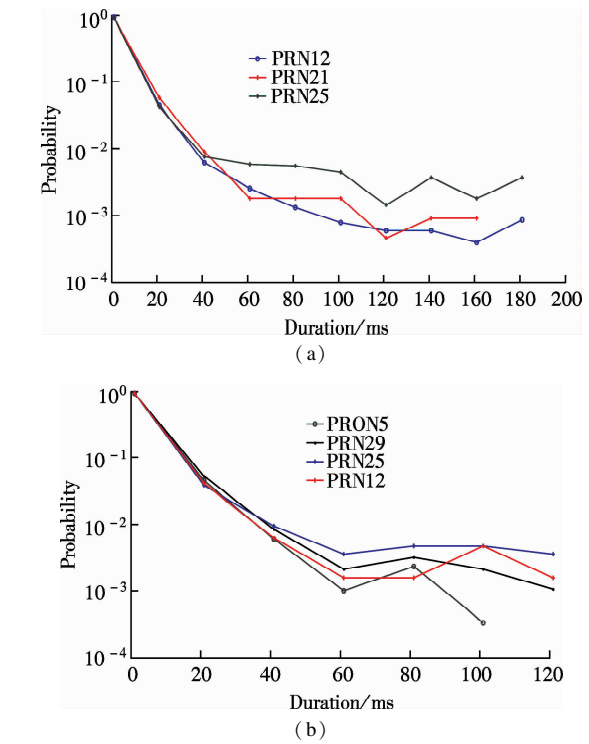


Fig. 3 Distributions of GPS L1 fading duration of signal intensity. (a) With the starting time of 0:00:01; (b) With the starting time of 23:00:02

important characteristics for GPS navigation. It is important to design a receiver having a short reacquisition time to reduce the probability of simultaneous loss of many satellites.

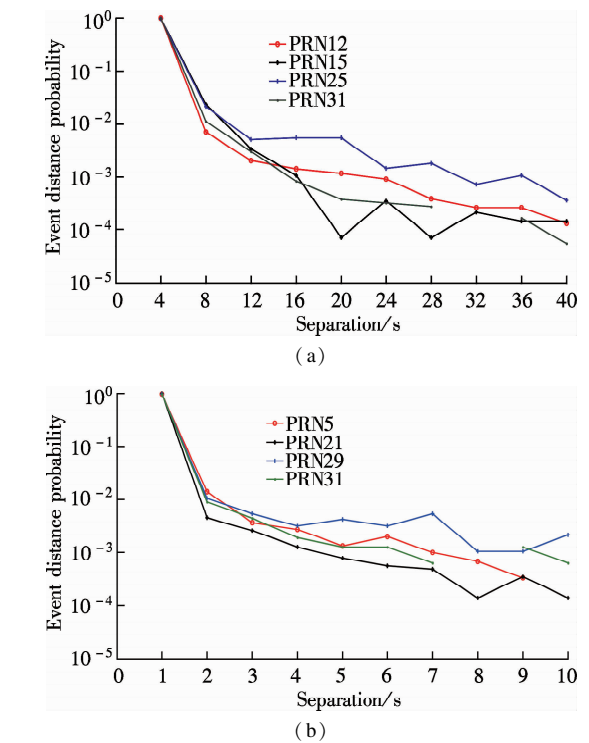


Fig. 4 Distributions of GPS L1 time separation between fades of signal intensity. (a) With the UTC starting time of 0:00:01; (b) With the UTC starting time of 23:00:02

The numbers of the signal intensity fading events under the thresholds of -10 and -15 dB are shown in Tab. 2, respectively. The Matlab is used as a simulation platform to analyze. It can be seen that the number of signal intensity fading events differs in time and PRNs. The PRN12 is influenced by the most severe ionospheric scintillation with 29 422 fading events under the threshold of -10 dB when the UTC starting time is 0:00:01.

Tab. 2 Fading numbers of signal intensity fading events

Threshold	UTC of 0:00:01		UTC of 23:00:02	
	-15 dB	-10 dB	-15 dB	-10 dB
PRN12	15 270	29 422	637	2 479
PRN21	2 223	7 180	844	2 746
PRN25	2 760	6 364	950	4 014

4 SDR Processing and PVT Navigation Results

The low-latitude GPS L1 signal intensity fading indices including fading duration, time separation between fades and the numbers of fading events and a custom software defined receiver (SDR) are analyzed in the following to obtain a PVT solution. Since the latitude is low for Brazil, the maximum of 10 ms coherent integration time combined with two non-coherent summations is used in signal acquisition to accumulate signal power so that the deep fades are compensated during strong scintillation. This is also important for the short reacquisition time of the SDR processing under frequent deep signal fading. The reacquisition time is designed to be 1.8 s in the real scintillation test.

A second-order PLL is implemented for carrier tracking. The phase error discriminator used in the PLL is a Costas discriminator. The code tracking loop is a conventional second-order delay lock loop (DLL). A normalized early minus late power envelope discriminator is used in the DLL. The pull-in time in carrier tracking is set to be 500 ms and the DLL pull-in noise bandwidth is set to be 2 Hz while PLL pull-in noise bandwidth is set to be 25 Hz. When the tracking loop is stabilized, the DLL noise bandwidth is set to be 1 Hz and the PLL noise bandwidth is set to be 10 Hz.

Figs. 5(a) and (b) shows that the GPS L1 signal PVT solutions are calculated by the customized software receiver, and they also show the positioning variations under the UTM(universal transverse mercator) coordinate and the receiver clock error. The east and north positioning variations are within 5 m which is much less than that in the upper direction, while the clock oscillator error is about -0.8×10^{-6} . The results show that the ionospheric scintillation effects are suppressed and the proposed SDR processing algorithms are proved to be efficient. The 3D plot position in the UTM system is shown in Fig. 5(c) and Fig. 5(d) shows the sky plot. The real position is at the red cross (Lat: $-23^{\circ}12'27.577\ 2''$,

Lng: $-45^{\circ}51'35.141\ 4''$, Hgt: $+693.4$) and the distribution of the positioning is concentrated. The satellites with PRN5, PRN12, PRN18, PRN21, PRN25, PRN29, PRN31 are in the sky and are analyzed in details in the above sections.

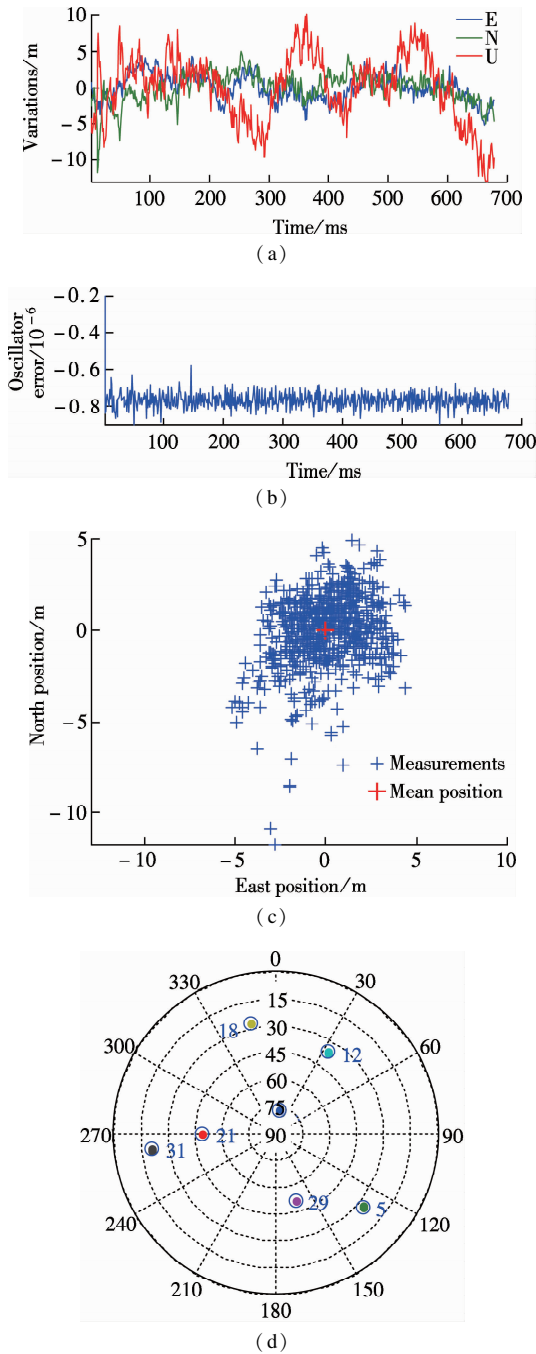


Fig. 5 GPS L1 signal PVT solution. (a) UTM coordinates variations; (b) Receiver clock error; (c) Positions in the UTM system (3D plot); (d) Sky plot

5 Conclusion

The ionospheric scintillation has a serious impact on GPS navigation measurements, so the GPS signal calculation accuracy is low. In this paper, the impact of ionospheric scintillation on GPS amplitude fading in Brazil is

analyzed, including fading duration, time separation between fades and the numbers of signal intensity fading events by setting two different fading thresholds of -15 and -10 dB. It is useful for signal reacquisition and GPS receiver signal processing to analyze the ionospheric scintillation. It is a promising way to build robust GPS receivers by using the selective fading phenomenon, which can maintain the lock of the tracking loop during strong ionospheric scintillation.

References

[1] Carroll M J. Advanced GPS receiver algorithms for assured navigation during ionospheric scintillation[D]. Miami, USA: Computational Science and Engineering, Miami University, 2014.

[2] Carroll M J, Morton Y J, Vinande E. Triple frequency GPS signal tracking during strong ionospheric scintillations over Ascension Island[C]//2014 IEEE/ION Position, Location and Navigation Symposium. Monterey, CA, USA, 2014: 43–49. DOI: 10.1109/PLANS.2014.6851356.

[3] Kassabian N, Morton Y J. Extending integration time for Galileo tracking robustness under ionosphere scintillation [C]//2014 IEEE/ION Position, Location and Navigation Symposium. Monterey, CA, USA, 2014: 59–72. DOI:10.1109/plans.2014.6851358.

[4] Akala A O, Doherty P H, Carrano C S, et al. Impacts of ionospheric scintillations on GPS receivers intended for equatorial aviation applications[J]. *Radio Science*, 2012, **47** (4): RS40071–RS400711. DOI: 10.1029/2012RS004995

[5] Wang J, Morton Y T. High-latitude ionospheric irregularity drift velocity estimation using spaced GPS receiver carrier phase time-frequency analysis[J]. *IEEE Transactions on Geoscience and Remote Sensing*, 2015, **53**(11): 6099–6113. DOI:10.1109/tgrs.2015.2432014.

[6] Seo J, Walter T, Chiou T Y, et al. Characteristics of deep GPS signal fading due to ionospheric scintillation for aviation receiver design [J]. *Radio Science* 2009, **44** (1): RS0A16-1–RS0A16-10. DOI:10.1029/2008rs004077.

[7] Liu D, Feng J, Deng Z X, et al. Ionospheric scintillation effects on GPS positioning performance [J]. *Chinese Journal of Radio Science*, 2010, **25**(4):702–710.

[8] Li G B, Zhu H, Shi W S. Influence of ionospheric scintillation on GPS capture performance[J]. *Ship Electronic Engineering*, 2012, **32**(12):55–57.

[9] Jiao Y, Morton Y, Taylor S, et al. Characteristics of low-latitude signal fading across the GPS frequency bands [C]//*Proceedings of ION GNSS*. Tempa, FL, USA 2014:1203–1212.

[10] Jiao Y, Morton Y T, Taylor S, et al. Characterization of high-latitude ionospheric scintillation of GPS signals[J]. *Radio Science*, 2013, **48**(6):698–708. DOI:10.1002/2013rs005259.

[11] Xu D, Morton Y. GPS carrier parameters characterization during strong equatorial ionospheric scintillation [C]//*Proceedings of ION ITM*. Dana Point, CA, USA, 2015:1–10.

[12] Xu D, Morton Y, Akos D, et al. GPS multi-frequency carrier phase characterization during strong equatorial ionospheric scintillation [C]//*Proceedings of ION GNSS*. Tampa, FL, USA, 2015: 1–10.

[13] Taylor S, Morton Y, Jiao Y, et al. An improved ionosphere scintillation event detection and automatic trigger for GNSS data collection systems [C]//*Proceedings of ION ITM*. Newport Beach, CA, USA 2012: 1563–1569.

[14] Zhang L, Morton Y. GPS carrier phase spectrum estimation for ionospheric scintillation studies[J]. *Navigation*, 2013,**60**(2):113–122. DOI:10.1002/navi.33.

低纬度地区 GPS 电离层闪烁信号幅度衰减特性分析

祝雪芬^{1,2} 陈熙源^{1,2} 黄浩乾^{1,2} 陈建锋³ 徐斌斌^{1,2}

(¹ 东南大学仪器科学与工程学院,南京 210096)

(² 东南大学微惯性仪表与先进导航技术教育部重点实验室,南京 210096)

(³ 江苏大学汽车工程研究院,镇江 212013)

摘要:针对低纬度地区强电离层闪烁发生时会造成接收的卫星信号幅度深度衰减,导致 GPS 跟踪环路失锁、定位误差增大甚至导航中断的问题,提出了一种基于多通道中频信号采集系统的 GPS L1 软件接收机在经历强电离层闪烁时的信号处理算法.首先,基于信号强度观测量得到的几万个衰减事件,分析了低纬度地区的幅度衰减特性,包括衰减时间、衰减间隔及衰减事件数,其中衰减阈值分别设为 -15 和 -10 dB.在 -15 dB 的衰减阈值下,主要衰减时间非常短,通常在 20 ms 以内,在 23:00~24:00 之间,主要衰减间隔小于 2 s.故需要设计的接收机应具有短的重捕时间,才能减少多个卫星同时失锁的可能性.然后用定制软件接收机来完成相关捕获、跟踪及 PVT(位置、速度、时间)解算.结果表明:分析低纬度地区电离层闪烁对 GPS 幅度衰减的影响,对于设计高级跟踪算法及提高 GPS 接收机的鲁棒性和精度将提供有益指导.

关键词:GPS L1; 电离层闪烁; 幅度衰减特性

中图分类号:TN967.1